

Spontaneous Breaking of Translational Invariance and Spatial Condensation in Stationary States on a Ring. II. The Charged System and the Two-Component Burgers Equations

Peter F. Arndt¹ and Vladimir Rittenberg²

Received January 30, 2001; accepted December 30, 2001

We further study the stochastic model discussed in ref. 2 in which positive and negative particles diffuse in an asymmetric, CP invariant way on a ring. The positive particles hop clockwise, the negative counter-clockwise and oppositely-charged adjacent particles may swap positions. We extend the analysis of this model to the case when the densities of the charged particles are not the same. The mean-field equations describing the model are coupled nonlinear differential equations that we call the two-component Burgers equations. We find roundabout weak solutions of these equations. These solutions are used to describe the properties of the stationary states of the stochastic model. The values of the currents and of various two-point correlation functions obtained from Monte-Carlo simulations are compared with the mean-field results. Like in the case of equal densities, one finds a pure phase, a mixed phase and a disordered phase.

KEY WORDS: Non-equilibrium statistical mechanics; phase transitions; Burgers equation.

1. INTRODUCTION

Phase transitions in stationary (far away from equilibrium) states present still many open questions. Some time ago,⁽¹⁾ we have introduced a simple one-dimensional three-state model which has interesting properties. In this

¹ Physics Department, University of California at San Diego, La Jolla, California 92093-0319; Institute for Theoretical Physics, University of California at Santa Barbara, Santa Barbara, California 93106-4030; e-mail: arndt@physics.ucsd.edu

² Department of Mathematics and Statistics, University of Melbourne, Parkville, Victoria 3010, Australia; Physikalisches Institut, Nußallee 12, 53115 Bonn, Germany.

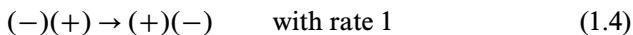
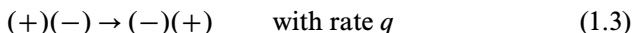
model one takes a ring with L sites, the positive particles hop clockwise with a rate λ :



((0) is a vacancy). The negative particles hop counter-clockwise with the same rate λ



and oppositely charged adjacent particles may exchange positions



This model is translational invariant and the numbers of positive and negative particles are conserved. A detailed study of this model was done in ref. 2 where we have considered the case in which the densities p (positive particles) and m (negative particles) were taken equal ($p = m = \rho$). Obviously

$$p + m + v = 1 \quad (1.5)$$

where v is the density of vacancies. Using mean-field analysis, Monte-Carlo simulations and representations of the quadratic algebra given by the rates describing the processes (1.1)–(1.4) we have shown that the model has three phases. For $q < 1$ (independent on λ and the densities) translational invariance is spontaneously broken (pure phase). In this phase, in the thermodynamical limit, the system organizes itself into a block of positive particles followed by a block of negative particles and one block of vacancies. All blocks are pinned in an arbitrary position on the ring. For $1 < q < q_c(\lambda, \rho)$ (called mixed phase) one has Bose–Einstein condensation in coordinate space (spatial condensation). In this phase one has again charge segregation but translational invariance is not broken. To understand better what happens (for finite but large L) it is interesting to start with the mean-field results. Neglecting fluctuations, the mean-field solutions, which break translational invariance, show two pinned adjacent blocks. One block (that we called condensate) contains only charged particles (no vacancies) with inhomogeneous distributions and a block (called fluid) which contains all the vacancies and where the particles have homogeneous distributions (see ref. 2, Fig. 25). As a result of fluctuations, the whole structure (condensate+fluid) makes a Brownian motion on the ring and the stationary probability distribution function is obtained taking with

equal probability, the two adjacent blocks anywhere on the ring. For $q > q_c$, one is in the disordered phase; there is no charge segregation and the particles are distributed uniformly. In mean-field, one gets:

$$q_c = 1 + \frac{4\lambda\rho}{1+2\rho} \quad (1.6)$$

and a remarkable simple expression for the current in the mixed phase:

$$j = (q-1)/4 \quad (1.7)$$

The current being independent on λ and ρ .

As shown by one of us,⁽³⁾ one can use the distributions of the zeroes of the partition function in the grand canonical ensemble as a function of fugacity à la Lee and Yang,⁽⁴⁾ in order to get good estimates of q_c (for other methods, see ref. 2).

The aim of this paper is to further study this model in the case of unequal densities. As we are going to see, the physics is different. Beside our physical motivation, we have also a mathematical one. The mean-field equations given by the present model, are coupled nonlinear differential equations and as we are going to show, we are able to find exact weak⁽⁵⁾ solutions of these equations. We believe that without knowing the physics of the model it would have been very difficult to guess them. Since in the absence of vacancies, the coupled equations reduce to the Burgers equation,⁽⁶⁾ we call the mean-field equations "The two-component Burgers equations." In ref. 2, for equal densities, we found stationary solutions of these equations. In the case of unequal densities we find new solutions of these equations. We have again three phases, now however, the spatial structure (which exists in the pure and mixed phases) drifts with constant velocity around the circle. In the large L limit, the drift velocity vanishes exponentially in the pure phase, like $1/L$ for $q = 1$ and is finite for $1 < q < q_c(\lambda, \rho, m)$. We think that finding new analytical solutions of PDE is important and it is possible that our approach can be used to solve other PDE.

From the mean-field results one can be tempted to conclude that one has no stationary solutions at all in the case of unequal densities even if we take into account fluctuations. Actually one can be left with this feeling from ref. 7 where a different model was considered. That stationary solutions exist in our problem is known from the existence^(1,2) of a quadratic algebra with known representations and one can obtain in this way exact solutions for the probability distribution for the stationary state.

In order to understand the physics of the problem it is instructive to have a look at the time evolution of a Monte-Carlo run which can be seen in Fig. 1. The parameters are chosen such that one is in the mixed phase.

One notices that at a given time t one has two regions. In one of them (the condensate), there are no vacancies and that the boundaries are sharp. This allows a definition of the width of the condensate: one takes the last vacancy seen in the simulation on the left side and the first vacancy seen on the right side. In the condensate the particles are not uniformly distributed: the positive ones are predominantly on the left side and the negative ones are on the right side. The second region (the fluid) contains all the vacancies and the charged particles are distributed at random. If we now look at the figure downwards, one notices that the condensate drifts to the left with a constant velocity which can be estimated following for example the last vacancy on the left side of the condensate. Notice also that in the fluid, the positive particles drift to the right whereas the negative particles drift to the left.

In Fig. 2 we show the average values of the drift velocities obtained looking at the motion of the condensate as a function of the size of the system L in the pure phase ($\lambda = 1$, $q = 0.8$), for $q = 1$ ($\lambda = 1$) and in the mixed phase ($\lambda = 1$, $q = 1.2$). We have taken $p = 0.4$ and $m = 0.1$.

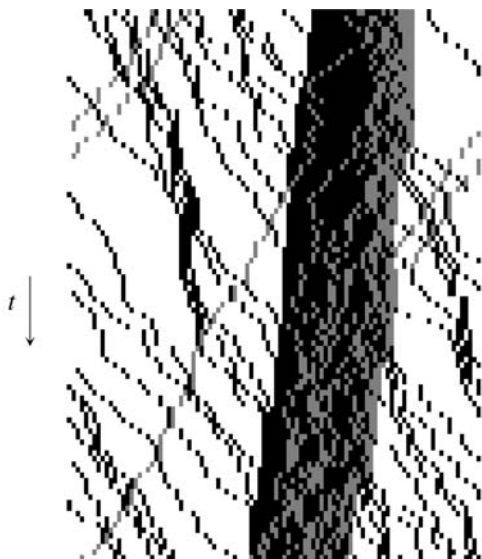


Fig. 1. A Monte-Carlo "film" for $q = 1.2$, $\lambda = 1$, $p = 0.3$, $m = 0.1$ (mixed phase), $L = 100$. The time t is running from the top to the bottom of the figure. The positive particles are depicted black, the negative ones-gray.

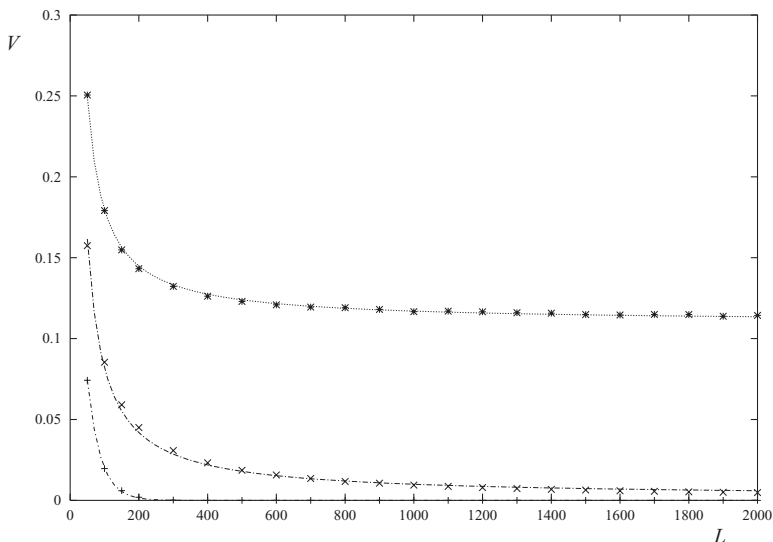


Fig. 2. The drift velocity V as a function of the size of the system L . The upper curve corresponds to the mixed phase, the intermediate one to $q=1$ and the lowest one to the pure phase.

In the pure phase, the velocity vanishes exponentially. A fit (also shown in Fig. 2) to the data gives:

$$V = 0.2742 \exp(-0.02615L) \quad (1.8)$$

For $q=1$, the drift velocity vanishes algebraically:

$$V = 9.602/L \quad (1.9)$$

whereas in the mixed phase the fit gives:

$$V = 0.116 + 6.9658/L \quad (1.10)$$

We now return to Fig. 1 and notice that the condensate does not only drift to the left but also does a Brownian motion. If one follows again the last vacancy on the left side of the condensate, it behaves like a random walker and therefore one can determine the diffusion coefficient D . This was done for different sizes of the system and the results are shown in Fig. 3 for the same parameters as those used in Fig. 2. We notice that similar to the drift velocity V , for large values of L , the diffusion coefficient converges to a constant value in the mixed phase, vanishes algebraically for $q=1$ and exponentially in the pure phase.

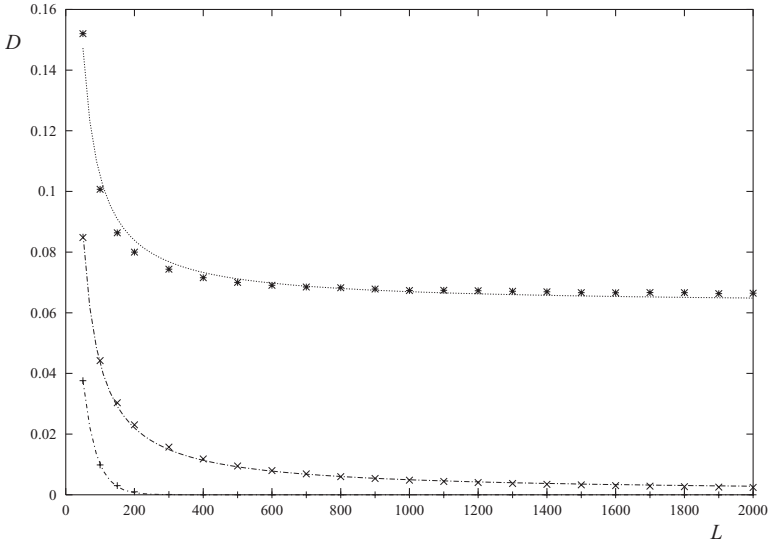


Fig. 3. The diffusion coefficient D as a function of the size of the system L . The upper curve corresponds to the mixed phase, the intermediate one for $q = 1$ and the lowest one to the pure phase.

We would like to stress that what we have described up to now is the time evolution of the fluctuating system (the drift velocity and the diffusion constant are not properties of the stationary state), nevertheless from our observations we can guess the properties of the stationary states. It is clear that in the pure phase, in the thermodynamical limit, one gets three adjacent pinned blocks and like in the case of equal densities, translational invariance is broken. The situation is different in the mixed phase. If we follow again the last vacancy on the left side of the condensate, since it moves like a random walker with a finite diffusion coefficient, the dispersion increases with time up to when it reaches the perimeter of the ring. For later times one can find this vacancy anywhere on the ring. This implies that in the stationary state, one finds with equal probability the structure condensate+fluid in any position on the ring. The existence of such a structure obviously implies charge segregation (long range correlations) without breaking of translational invariance.

We can understand better now what is going to be the role of mean-field calculations. On one hand, one can estimate non-equilibrium quantities like the drift velocity, on the other hand one can obtain the condensate+fluid structure. Once the latter is known, one can obtain the probability distribution of the stationary state taking as mentioned, with equal probability the charge distribution obtained in mean-field in any position on the ring.

The paper is organized as follows. In Section 2 we consider the mean-field equations for the case $q > 1$. Those are the two-component Burgers equations. In this section we shortly remind the reader some of the results obtained in ref. 2 for the case of equal densities and also present some new ones. In Section 3 we find exact weak solutions of the two-component Burgers equations for the case of unequal densities which tell us under which conditions the condensation phenomenon appears. In this way one can obtain the function $q_c(\lambda, p, m)$. Moreover one obtains the drift velocity V and the charge distributions in the condensate. Let us stress that unlike the Burgers equation one can't obtain the solutions with a drift from the stationary ones. We have not considered the case $q < 1$ since it can be studied along similar lines (see ref. 2 for the case $p = m$).

In Section 4 we discuss the properties of the stationary states taking into account fluctuations. One presents data on the currents and correlation functions obtained from Monte-Carlo simulations and compares them with the results obtained in mean-field used as described above. We also give some results using the algebraic approach⁽²⁾ which is, in the case of unequal densities, harder to apply. The conclusion is presented in Section 5.

Since this work is the continuation of the one presented in ref. 2, this paper is not self-contained and it can't be understood without first reading ref. 2 unless one is interested only in the solutions of the two-component Burgers equations described in Sections 2 and 3.

We would like to mention that the model described above was subsequently studied again on a ring, in the case in which only one vacancy (seen as a defect) is present⁽⁷⁾ and for a special case of open boundaries.⁽⁸⁾

2. THE TWO-COMPONENT BURGERS EQUATIONS ($q > 1$)

The mean-field equations in the continuum of the model defined by Eqs. (1.1)–(1.4) are (ref. 2, Appendix B):

$$\frac{\partial j_{\pm}}{\partial x} \pm \frac{\partial \rho_{\pm}}{\partial t} = 0 \quad (2.1)$$

where ρ_{\pm} are the local densities of the charged particles (ρ_0 is the local density of the vacancies) satisfying the obvious relation:

$$\rho_+ + \rho_- + \rho_0 = 1 \quad (2.2)$$

j_+ is the local current density of positive particles, j_- is minus the local current density of negative particles (the minus sign is convenient if one looks at stationary states in the case of equal densities since with this choice of signs one gets $j_+ = j_-$). The expressions of the current densities are:

$$j_{\pm} = \lambda \rho_{\pm} \rho_0 + (q-1) \rho_+ \rho_- + \frac{1}{2} \left[(q+1) \left(\rho_+ \frac{\partial \rho_-}{\partial x} - \rho_- \frac{\partial \rho_+}{\partial x} \right) \pm \lambda \left(\rho_{\pm} \frac{\partial \rho_0}{\partial x} - \rho_0 \frac{\partial \rho_{\pm}}{\partial x} \right) \right] \quad (2.3)$$

We are looking at periodic solutions of the Eqs. (2.1):

$$\rho_{\pm}(x, t) = \rho_{\pm}(x + L, t) \quad (2.4)$$

where L is the perimeter of the ring. We will also be interested in solutions with a drift velocity V counter clockwise (see Fig. 1):

$$\rho_{\pm}(x, t) = \rho_{\pm}(x + Vt) \quad (2.5)$$

which implies that in the moving frame, the quantities

$$C_{\pm} = \pm V \rho_{\pm} + j_{\pm} \quad (2.6)$$

are independent of x . It is useful to define

$$y = \frac{x}{L}, \quad 0 \leq y \leq 1 \quad (2.7)$$

and

$$J_{\pm} = \frac{C_{\pm}}{q-1}, \quad W = \frac{V}{q-1}, \quad \ell_{\pm} = \frac{j_{\pm}}{q-1}, \quad (2.8)$$

$$v = \frac{q+1}{2L(q-1)}, \quad \eta = \frac{\lambda}{q-1}, \quad \mu = \frac{\eta}{2L}$$

In Eq. (2.8) we have assumed that $q > 1$. Rescaling the time, instead of Eqs. (2.1), (2.3)–(2.6) one finds:

$$\frac{\partial \ell_{\pm}}{\partial y} \pm \frac{\partial \rho_{\pm}}{\partial t} = 0 \quad (2.9)$$

$$\ell_{\pm} = \eta \rho_{\pm} \rho_0 + \omega \rho_+ \rho_- + v \left(\rho_+ \frac{\partial \rho_-}{\partial y} - \rho_- \frac{\partial \rho_+}{\partial y} \right) \pm \mu \left(\rho_{\pm} \frac{\partial \rho_0}{\partial y} - \rho_0 \frac{\partial \rho_{\pm}}{\partial y} \right) \quad (2.10)$$

$$\ell_{\pm}(y, t) = \ell_{\pm}(y + 1, t) \quad (2.11)$$

$$\ell_{\pm}(y, t) = \ell_{\pm}(y + Wt) \quad (2.12)$$

$$J_{\pm} = \pm W \rho_{\pm} \pm \ell_{\pm} \quad (2.13)$$

where $\omega = 1$. Since the numbers of positive and negative particles are conserved, we are looking for solutions for given densities p and m :

$$\int_0^1 \rho_+ dy = p, \quad \int_0^1 \rho_- dy = m \quad (2.14)$$

We call the Eqs. (2.10)–(2.11) the two-component Burgers equations. We have coined this name to the equations since if the density of vacancies ρ_0 is equal to zero, we can make in Eqs. (2.10) the substitution

$$l_{\pm} = \frac{1}{2} \pm f \quad (2.15)$$

and see that f satisfies the Burgers equation⁽⁶⁾

$$\frac{\partial f}{\partial t} = \nu \frac{\partial^2 f}{\partial y^2} + \zeta f \frac{\partial f}{\partial y} \quad (2.16)$$

where $\zeta = 2$ and ν is the damping constant whose physical interpretation in our model can be read of from Eq. (2.8). One notices that in the infinite volume limit, the damping constant vanishes and one obtains the inviscid Burgers equation.⁽⁶⁾ The constant μ appearing in Eqs. (2.10) will be called moisture constant. Notice (see Eq. (2.8)) that the moisture constant also vanishes in the large L limit.

An important result of our investigation is that one is able to give exact solutions to the two-component Burgers equation. Let us review the results obtained in ref. 2 (Section 6). For equal densities, in the mixed phase, inspired by the results obtained numerically (see Fig. 25), one can obtain the stationary solutions in the following way. We divide the segment $0 < y < 1$ into two smaller segments: $0 < y < a$ where we have a condensate (no vacancies) with a non-uniform distributions of the charged particles and a second segment of length b , ($a + b = 1$) where the particles have a uniform distribution (fluid). Therefore in the condensate one can use the Burgers equation whereas in the fluid one has almost nothing to compute. Numerical investigation teach us how to sew the two segments: the density of positive particles is smooth at the right-side of the condensate ($y = a$) but not at the left-side ($y = 0$) where it is discontinuous. For the negative particles the discontinuity is at $y = a$ as a consequence of the CP invariance of the problem. The solutions obtained in this way are weak solutions of the differential equations which correspond to taking the moisture constant μ equal to zero. They represent an excellent approximation not only of the concentration profiles obtained numerically for the mean-field equations but also of the concentration profiles seen in computer simulations (see Figs. 8 and 9 in ref. 2).

The values of a are dependent on v , η and the density $p = m = \rho$. The domain in the space of the variables v , η , and ρ where solutions exist define the mixed phase. In the thermodynamic limit ($v = 0$) one obtains for b the value

$$B = \frac{v(1+2\eta)}{2(1+\eta)} \quad (2.17)$$

The result mentioned in Section 1 for q_c (see Eq. (1.6)) is obtained from Eq. (2.17) when takes $B = 1$ (the condensates disappears). To the results obtained in ref. 2 we would like to add some supplementary data which are relevant also for the case of unequal densities. For a given value of η there is a maximum value of v (v_{\max}) beyond which the condensation does not take place anymore. Moreover, one would expect that for v_{\max} the length of the condensate a is zero and that a increases as the damping constant decreases. This is not the case: for $v = v_{\max}$ one gets a non-vanishing value for a equal to a_{\min} .

In Figs. 4 and 5 one can see this phenomenon. We work with the variables q , λ and L instead of v and η (three variables instead of two) not only because our physical intuition is in these variables but also because in Section 4 we will look into the stochastic problem where, unlike in mean-field with $\mu = 0$, one has all the three variables.

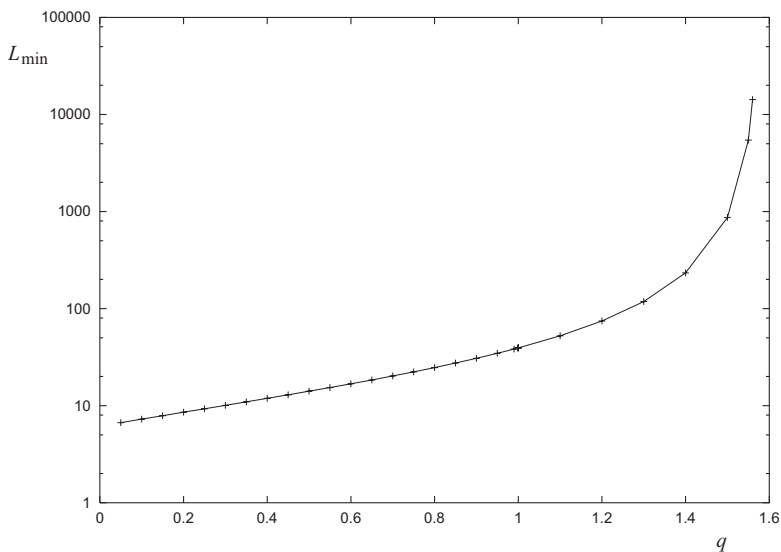


Fig. 4. The minimal length of the system to have a condensate for different q and $\lambda = 1$, $p = m = 0.2$. The data is very good fitted by $L = 17(q_c - q)^{-3/2}$.

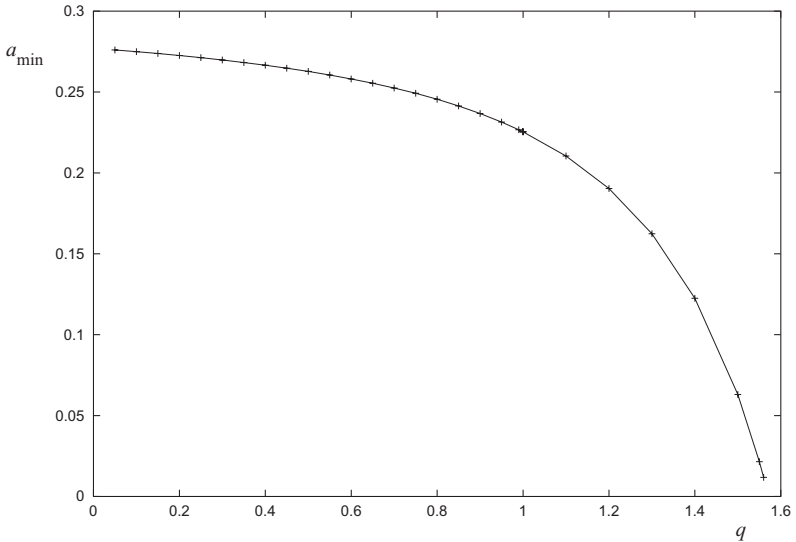


Fig. 5. The length of the condensate when condensation starts for different q and $\lambda = 1$, $p = m = 0.2$.

One notices that as we approach the critical point ($q_c = 1.5714$ as obtained from Eq. (1.6)), the minimal length L_{\min} diverges and the smallest condensate a_{\min} vanishes.

We should stress again that the solutions described above are weak solutions for the stationary states of the two-component Burgers equation. The current is constant on the segment $0 < y < 1$ but the densities are discontinuous. One can ask the question how do these discontinuous solutions look like if one looks at the “microscopic” problem on the lattice both in mean field and in Monte-Carlo simulations. As one can see in ref. 2, Fig. 25 or in the present paper Figs. 1 and 7, there are two dramatic changes in the densities over not more than a few sites for any lattice size L . If one works with the $y = x/L$ variable, these localized, abrupt, changes lead to discontinuous solutions.

One can ask if in the mixed phase the condensate+fluid solutions are the single ones. The answer is no. Obviously one has a solution where all the densities are constant (pure fluid). More interestingly, for a given value of v , η and ρ one can have solutions with n condensates (fluid + condensate + \dots + fluid + condensate) all of them with the same distribution of charged particles and located anywhere on the ring. It is easy to show that in order to get the solutions with n condensates one has to use the solutions obtained for a single condensate in which we take the damping constant

equal to nv . We didn't study the problem of the stability of these solutions. What we do know is that we have also obtained numerically these solutions by using the time-dependent mean field equations (see ref. 2, Eq. (B2)) and that we have obtained, depending on the initial conditions, solutions with no condensate, with one condensate and with two condensates. We didn't take large lattices where one could have seen more than two condensates.

One comment is in place concerning the multi-condensate solutions of mean-field. In the presence of fluctuations, each condensate behaves like a random walker who sooner or later will meet another random walker. When two condensates meet, they melt into a single condensate so that if one starts with n condensates, we end up with a single one. This is seen in Monte-Carlo simulations.

3. ROUNDABOUT SOLUTIONS OF THE TWO-COMPONENT BURGERS EQUATIONS ($q > 1$)

Before describing roundabout solutions of the differential equations (2.9) obtained in the case of unequal densities for the positive and negative particles, it is interesting to give some results obtained looking at large time solutions of the mean-field equations on the lattice (ref. 2, Eq. (B2)) obtained numerically. We are interested in the results obtained on the lattice for two reasons. Firstly, the physical problem is defined on the lattice and not in the continuum and we want to be sure that one obtains the same results. Secondly, we will solve the differential equations taking the moisture constant μ (see Eq. (2.8)) equal to zero, this implies looking for weak solutions, and it is important to know if the weak solutions reproduce the lattice results. If we take $q = 1.2$, $\lambda = 1$, $p = 0.4$, $m = 0.1$, and 1000 sites, we can plot the measured current densities versus the measured densities as shown in Fig. 6. One notices that in agreement with Eq. (2.6) one obtain straight lines. Moreover one can determine in this way, with high precision, the drift velocity V , its value for the parameters given above being $V = 0.11878$. The same value will be obtained later in the continuum (see Eq. (3.31) and is compatible with the fit to the Monte-Carlo data (see Eq. (1.10)) from which one obtains $V = 0.123$.

In Fig. 7 we show the distributions of the current densities and of the particle densities for a shorter lattice ($L = 200$) keeping all the other data unchanged. Like in the case of equal densities, one observes a condensate (a region without vacancies) and a fluid with uniformly distributed charged particles. Based on these numerical observations one can start to look for roundabout solutions of Eqs. (2.9), taking into account Eqs. (2.11)–(2.14). We first start with the condensate ($0 < y < a$) where we have no vacancies. Denoting

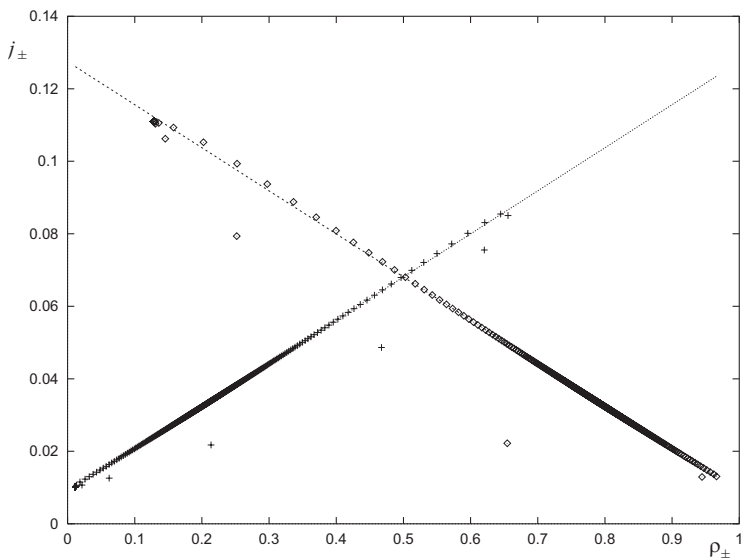


Fig. 6. The current densities as a function of the densities for $q = 1.2$, $\lambda = 1$, $L = 1000$, $p = 0.4$, $m = 0.1$ (lattice mean-field results). Using Eq. (2.6) one finds $V = 0.11878$.

$$\rho_{\pm}^c = \frac{1+W}{2} \pm u \quad (3.1)$$

$$J = \frac{J_+ + J_-}{2} \quad (3.2)$$

from Eq. (2.13) we obtain:

$$J_+ - J_- = W \quad (3.3)$$

and from Eqs. (2.13) and (2.10) we get:

$$\alpha^2 = 4J - 1 - W^2 = -4 \left(u^2 + v \frac{\partial u}{\partial y} \right) \quad (3.4)$$

We have denoted by ρ_{\pm}^c the densities of the charged particles in the condensate. Obviously

$$\rho_+^c + \rho_-^c = 1 \quad (3.5)$$

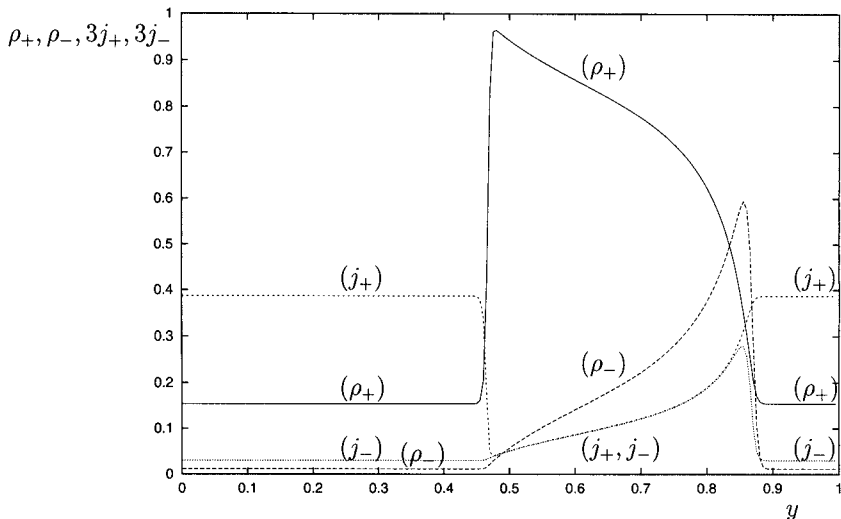


Fig. 7. The profiles of the densities and currents (scaled by a factor 3) obtained numerically on a lattice with 200 sites. The other data are like in Fig. 6. The condensate is drifting to the left.

We can integrate Eq. (3.4) and find:

$$u = \beta v \tan[\beta(a\varphi - y)] \quad (3.6)$$

where φ is an arbitrary constant and

$$\beta = \frac{\alpha}{2v} \quad (3.7)$$

At this point J , W , and φ are unknown constants which still have to be fixed. We now consider the fluid ($a < y < 1$) where all the vacancies are concentrated. In this domain the densities ρ_{\pm}^{n} and ρ_0^{n} are constant (independent of y) and verify the relation:

$$\rho_+^{\text{n}} + \rho_-^{\text{n}} + \rho_0^{\text{n}} = 1 \quad (3.8)$$

We obviously have

$$\rho_0^{\text{n}} = v/b \quad (3.9)$$

where v is the density of vacancies and b the length of the fluid. From Eq. (2.10) we get:

$$\ell_{\pm}^{\text{n}} = \eta \rho_{\pm}^{\text{n}} \rho_0^{\text{n}} + \rho_{\pm}^{\text{n}} \rho_{\mp}^{\text{n}} \quad (3.10)$$

We denote

$$\Delta = \rho_{+}^{\text{n}} - \rho_{-}^{\text{n}} \quad (3.11)$$

and get

$$W = \eta \Delta \rho_0^{\text{n}} \quad (3.12)$$

and

$$\alpha^2 = -\Delta^2(\eta - 1)^2 - (\rho_0^{\text{n}})^2(2\eta - 1) + 2\rho_0^{\text{n}}(\eta - 1) \quad (3.13)$$

We now sew the condensate with the fluid asking for the following conditions to be fulfilled:

$$\rho_{+}^{\text{c}}(a) = \rho_{+}^{\text{n}}, \quad \rho_{-}^{\text{c}}(0) = \rho_{-}^{\text{n}} \quad (3.14)$$

Using Eqs. (3.1) and (3.14) we get:

$$u(0) = \frac{1}{2} - \frac{W}{2} - \rho_{-}^{\text{n}}, \quad -u(a) = \frac{1}{2} + \frac{W}{2} - \rho_{+}^{\text{n}} \quad (3.15)$$

and therefore:

$$\rho_0^{\text{n}} = \beta v (\tan[\beta a(1 - \varphi)] + \tan[\beta a \varphi]) \quad (3.16)$$

and

$$W - \Delta = \beta v (\tan[\beta a(1 - \varphi)] - \tan[\beta a \varphi]) \quad (3.17)$$

We now use Eq. (2.14) and get for n condensates:

$$n \int_0^a \rho_{+}^{\text{c}} dy + \rho_{+}^{\text{n}} b = p, \quad n \int_0^a \rho_{-}^{\text{c}} dy + \rho_{-}^{\text{n}} b = m \quad (3.18)$$

It is useful to denote

$$d = p - m \quad (3.19)$$

and from Eq. (3.18) we obtain:

$$d = \left(Wa + 2 \int_0^a u \, dy \right) n + \Delta b \quad (3.20)$$

We have to make again a change of notations:

$$\beta a \varphi = \frac{\pi}{2} - \psi_1, \quad \beta a (1 - \varphi) = \frac{\pi}{2} - \psi_2 \quad (3.21)$$

In the new notations Eqs. (3.16), (3.17), (3.20), and (3.13) become:

$$\rho_0^{\text{fl}} = (\pi - (\psi_1 + \psi_2)) \frac{v}{a} [\cot \psi_2 + \cot \psi_1] \quad (3.22)$$

$$\Delta(\eta - 1) = (\pi - (\psi_1 + \psi_2)) \frac{v}{a} [\cot \psi_2 - \cot \psi_1] \quad (3.23)$$

$$d - \Delta(\eta - (\eta - 1) b) = 2vn \log \left(\frac{\sin \psi_2}{\sin \psi_1} \right) \quad (3.24)$$

$$\frac{4v^2}{a^2} (\pi - (\psi_1 + \psi_2))^2 = -\Delta^2(\eta - 1)^2 - (\rho_0^{\text{fl}})^2 (2\eta - 1) + 2\rho_0^{\text{fl}}(\eta - 1) \quad (3.25)$$

Taking into account Eq. (3.9), the four unknown b , ψ_1 , ψ_2 , and Δ can be obtained from the four equations (3.22)–(3.25) once p and m are given. In this way one can determine the profiles of densities in the condensate and the fluid, the currents and the drift velocities once we give η , v , p , and m . We have not determined the domain of these variables where the solutions exist. Having in mind the stochastic process where we have used the mean-field solutions in order to explain the properties of the stationary distributions, we have just looked at the values $q = 1.2$, $\lambda = 1$, $p = 0, 4$, and $m = 0.1$ in the mixed phase. As mentioned already before, and as can be seen from the equations given above, if we know the solutions for one condensate for any value L , one can obtain the solutions of the problem for n condensates for a lattice size L taking the solution for one condensate for a lattice of size L/n .

In Fig. 8 we show the drift velocities for the condensates which appear up to $L = 1000$. One notices first that the first condensate appears for $L = 60$. This implies that that one obtains n condensates when (roughly) $L > 60n$. Next one can see that for a given value of L many condensates move faster than fewer ones.

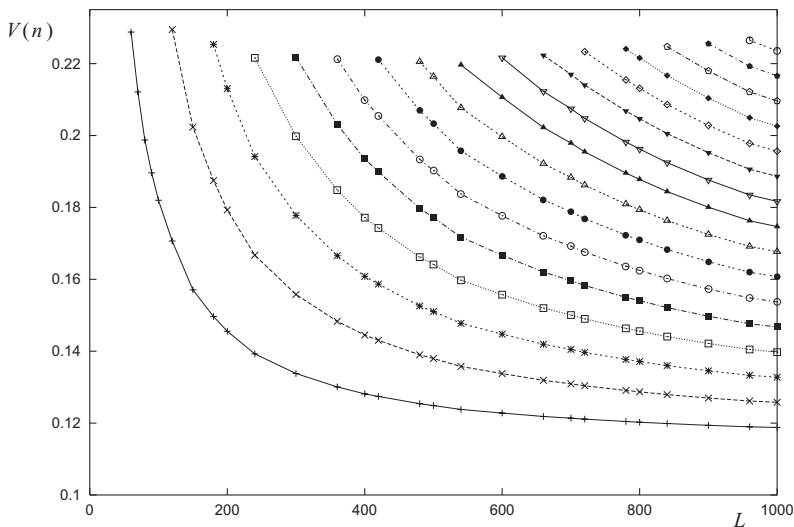


Fig. 8. The drift velocity $V(n)$ for the n -th condensate for $q = 1.2$, $\lambda = 1$, $p = 0.4$, $m = 0.1$, and $n = 1, 2, \dots, 16$ (from bottom to top). The first condensate appears for $L > 60$. The maximal drift velocity is about 0.23.

Various applications to the stochastic process of the distributions of the charged particles obtained solving the transcendental equations given above can be found in Section 4 (see Figs. 11 and 12).

The calculations simplify in the large L limit when the friction constant ν constant is small. Denoting the limiting values by

$$b \rightarrow B, \quad \Delta \rightarrow D, \quad \nu \rightarrow 0 \tag{3.26}$$

and

$$C = (\eta - 1) B \tag{3.27}$$

we obtain

$$\psi_1 = \frac{2\pi\nu(\eta - 1)}{1 - B} \left[\frac{v}{C} - D \right]^{-1}, \quad \psi_2 = \frac{2\pi\nu(\eta - 1)}{1 - B} \left[\frac{v}{C} + D \right]^{-1} \tag{3.28}$$

and

$$D = \frac{d}{\eta - C}, \quad \rho_0^n = \frac{v}{B} \tag{3.29}$$

C can be determined from the cubic equation

$$C^3 - C^2 \left[2\eta + \frac{v}{2}(\eta - 1) + \frac{d^2}{2v} \right] + C\eta[\eta + v(2\eta - 1)] - \frac{\eta^2 v}{2}(2\eta - 1) = 0 \quad (3.30)$$

We have used the equations (3.29) and (3.30) in the case $q = 1.2$, $\lambda = 1$, $p = 0.4$, and $m = 0.1$ and have obtained

$$\begin{aligned} V &= 0.11180, & B &= 0.57929, & D &= 0.11181 \\ \rho_0^n &= 0.86313 \\ j_+^n &= 0.1076, & j_-^n &= 0.0111, & j_+^c &= j_-^c = 0.03437 \end{aligned} \quad (3.31)$$

Notice that the value obtained this way for V is closed to the value determined numerically on the lattice as given in the caption of Fig. 6. As we are going to explain in Section 4, the average values of the current densities over the ring are very useful. In the large L limit they are given by

$$\langle j_{\pm} \rangle = (1 - B) j_{\pm}^c + B j_{\pm}^n \quad (3.32)$$

Using the values given in (3.31), one obtains:

$$\langle j_+ \rangle = 0.07678, \quad \langle j_- \rangle = 0.0288 \quad (3.33)$$

These values are going to be used in Section 4.

The case $q = 1$ can be studied in a similar way. For the drift velocity one finds:

$$V = \lambda x / L(p + m) \quad (3.34)$$

where x is given by

$$\frac{p - m}{p + m} = \frac{e^x + 1}{e^x - 1} - \frac{2}{x} \quad (3.35)$$

Taking $p = 0.4$, $m = 0.1$, and $\lambda = 1$, we get $V = 9.602/L$ in excellent agreement with the results obtained in the Monte-Carlo simulations (1.9). Obviously the case $q < 1$ can also be solved analytically (the trigonometric functions appearing for example in Eq. (3.6) change into hyperbolic ones).

4. THE MIXED PHASE. COMPARISON BETWEEN MEAN-FIELD RESULTS AND MONTE-CARLO SIMULATIONS

In the last two sections we have shown, the mean-field equations related to the stochastic process defined by Eqs. (1.1)–(1.4). In ref. 2 we

have discussed in detail, in the case of equal densities, how to use mean-field in order to explain the properties of the stationary states. One assumes that in the mixed phase, one can take with equal probability in any position of the ring the structure (condensate + fluid) obtained in mean-field. In this section we extend this discussion for the case of unequal densities. We limit ourselves to the case $p = 0.4$, $m = 0.1$, and $\lambda = 1$ only.

In Fig. 9 we give the average values of the currents $\langle j_+ \rangle$ and $\langle j_- \rangle$, for $q = 1.2$ and various lattice sizes. Within the errors they look like they converge to the large L limit obtained in mean-field. Since in mean-field the current-densities are not constant (see Fig. 7), one has to compute the average value of the current densities j_+ and j_- on the ring. For $q > 1$, in the infinite L limit only, the calculation of the averages is again simple since in the condensate the positive and negative particles have a uniform distribution like in the fluid (see also Eqs. (3.32)–(3.33)). The calculation is more complicated in the case of large but finite values of L .

The average values of the currents for various values of q are shown in Fig. 10. The mean-field values are obtained as described above, the Monte-Carlo values are obtained using results from finite lattices and extrapolating to L infinity. Similar to the case of equal densities, the currents are very well given by mean-field up to a value q_c (around 1.6). This is the mixed phase. For $q > q_c$ the currents have a different behavior (one is in the disordered phase).

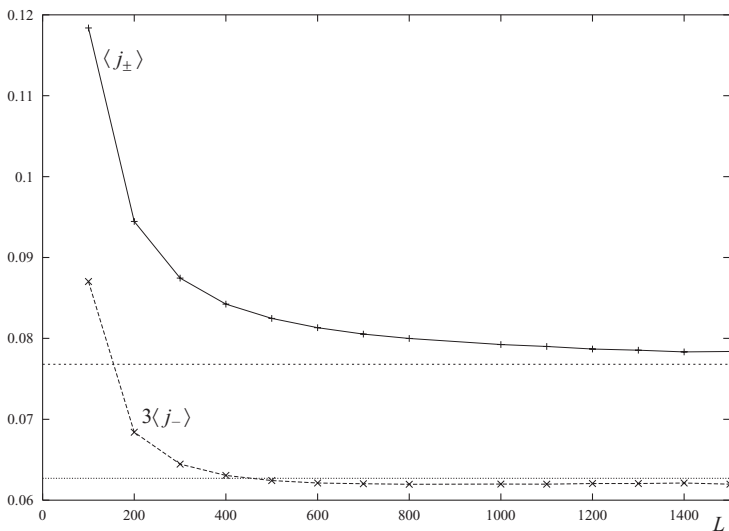


Fig. 9. $\langle j_+ \rangle$ and $3\langle j_- \rangle$ from Monte-Carlo data for $q = 1.2$, $\lambda = 1$, $p = 0.4$, $m = 0.1$. The lines come from mean-field in the $L \rightarrow \infty$ limit.

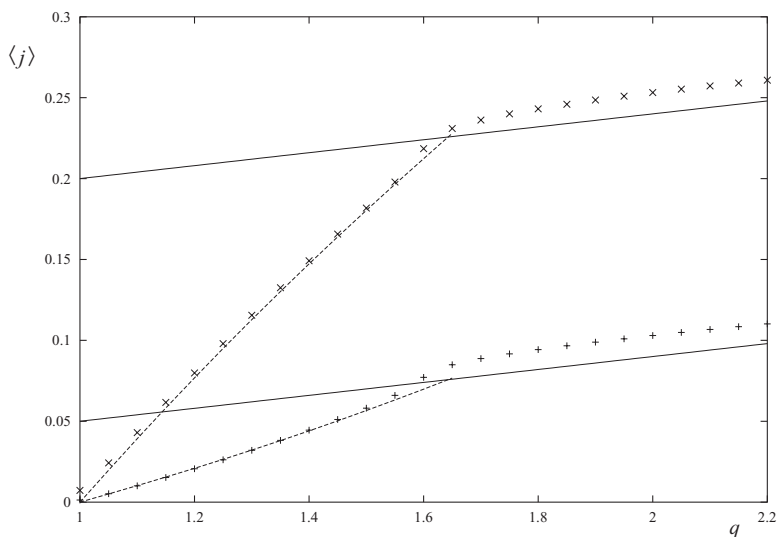


Fig. 10. The current of positive (top), negative particles (bottom) from Monte-Carlo Simulations and from mean-field calculations in the limit $L \rightarrow \infty$ (dashed lines) and homogeneous mean-field (solid lines). The parameters are $\lambda = 1$, $p = 0.4$, $m = 0.1$, and $L = 800$.

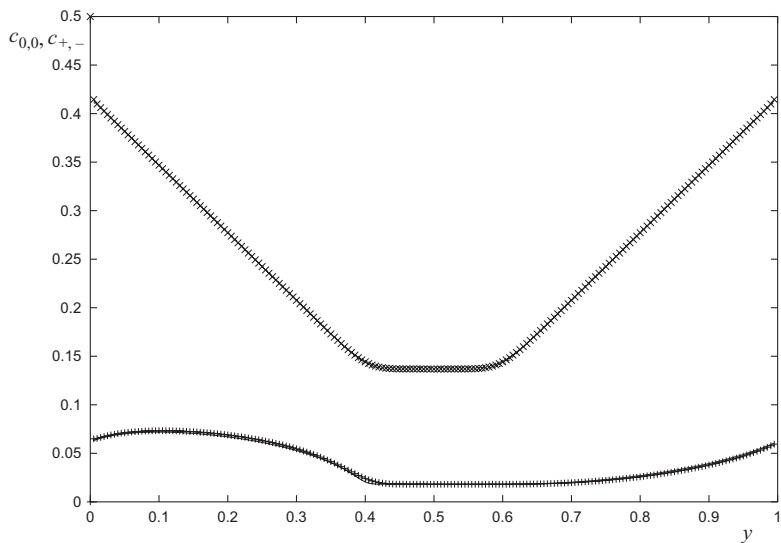


Fig. 11. The correlation functions $c_{0,0}$ (top) and $c_{+,-}$ (bottom) for $q = 1.2$, $\lambda = 1$, $p = 0.4$, $m = 0.1$, and $L = 200$. Each curve consists of the Monte-Carlo and mean-field data lying perfectly upon each other.

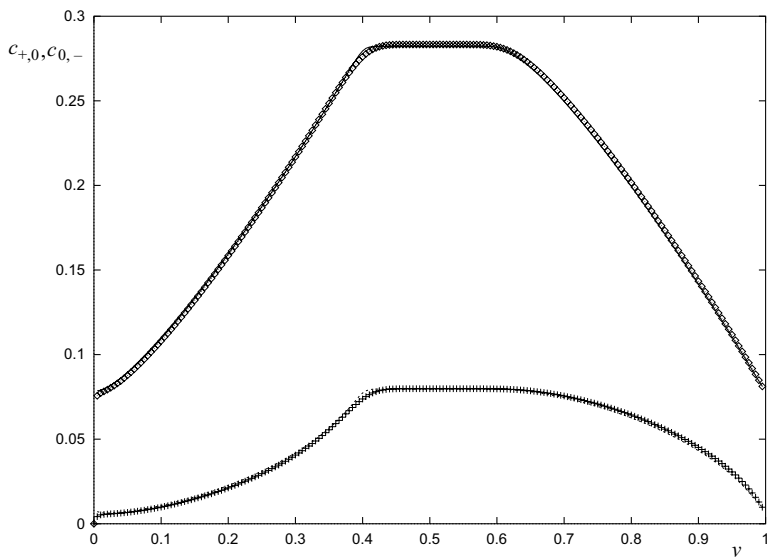


Fig. 12. The correlation functions $c_{+,0}$ (top) and $c_{0,-}$ (bottom) for $q = 1.2$, $\lambda = 1$, $p = 0.4$, $m = 0.1$, and $L = 200$. Each curve consists of the Monte-Carlo and mean-field data lying perfectly upon each other. The drift velocity is $\lambda \lim_{y \rightarrow 0} (c_{+,0} - c_{0,-}) / (1 - p - m)$. For equal densities all four curves are lying on top of each other.

In Figs. 11 and 12 and we show the two-point correlation functions as a functions of the distance $R = yL$ obtained in Monte-Carlo simulations ($L = 200$) and in mean-field. In the case of correlation functions, in order to obtain the mean-field results one had to use the results of Section 3 for $L = 200$. The agreement between the simulations data and the mean-field results is remarkable.

Since one is in a stationary state, one can't talk about drift velocities which are seen in non-equilibrium or in the roundabout solutions of the mean-field equations. Let us observe however that when we use the mean-field results in order to derive the correlation functions given in Fig. 12, for small values of y , one obtains the following value of the drift velocity V

$$V = \lambda \lim_{y \rightarrow 0} \frac{c_{+,0} - c_{0,-}}{1 - p - m} \quad (4.1)$$

This expression is so simple because in this limit, only the fluid and not the condensate plays a role. Using the results of the Monte-Carlo simulations and Eq. (4.1) one can estimate the drift velocity. One gets $V = 0.14$ which is perfectly consistent with the value obtained looking at the random movement of the condensate (see Figs. 2 and 13).

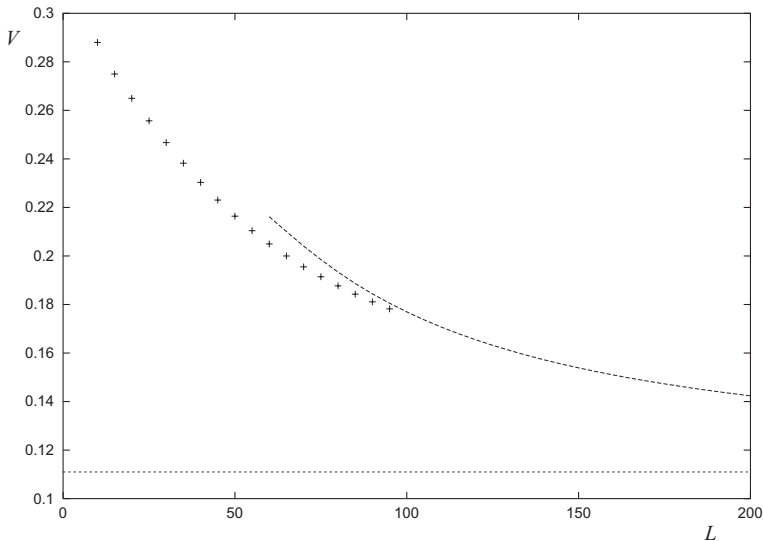


Fig. 13. The “drift velocity” for $q = 1.2$, $\lambda = 1$, $p = 0.4$, $m = 0.1$ from the algebraic approach $V = (\langle j_+ \rangle - \langle j_- \rangle) / (1 - p - m)$ (points) and Monte-Carlo simulations (line). The straight line gives the mean-field value for the limit $L \rightarrow \infty$.

Up to now we have discussed only the Monte-Carlo data. In ref. 2 we have also shown how to use the algebraic approach in order to obtain the current using the grand canonical ensemble (for correlation functions this approach gives wrong results). In the case of unequal densities one has to deal with two chemical potentials and the calculations become difficult. It is interesting to consider the quantity

$$V = \frac{\langle j_+ \rangle - \langle j_- \rangle}{1 - p - m} \quad (4.2)$$

defined for the stationary state. In mean-field, V as defined by Eq. (4.2), is indeed the drift velocity (use Eq. (2.6) and compute C_{\pm} in the fluid). In Fig. 13 we give the values of V , as defined by Eq. (4.2), obtained for small lattices and compare them with the mean-field results. We also show the values of V obtained in Monte-Carlo simulations (those are not data describing the stationary states!) and presented already in Fig. 2. Notice that we have mentioned a fourth way to estimate V (see Eq. (4.1)) for which we have obtained only one value for $L = 200$ which also is compatible with the data of Fig. 13. The compatibility of the various ways to estimate the drift velocity makes us believe that we have understood at least part of the physics of the mixed phase.

5. CONCLUSION

In this sequel of ref. 2 we have introduced what we call the two-component Burgers equations defined by Eqs. (2.9) and (2.10). These equations correspond to the mean-field approximation of the stochastic model defined in Section 1. We have found roundabout a weak solutions of these equations for $\omega = 1$ in Section 3. This case correspond to the mixed phase of the stochastic model. The weak solution of the two-component Burgers equations is obtained if we take the moisture constant $\mu = 0$ in these equations. When compared with the solutions of the equations when the moisture constant is not zero, which can be obtained numerically, one sees that one gets a very good approximation.

The analytical roundabout solutions presented in Section 3 allow to determine the domain in the parameter space where the mixed phase exists. Moreover, using these solutions one can obtain predictions for the stochastic problem as explained in Section 4. These predictions are in good agreement with the results of Monte-Carlo simulations on large lattices, also for the case in which the densities of positive and negative particles are not equal. Since Monte-Carlo simulations are much time-consuming, in the present paper we have performed a less careful analysis of the data as compared with the case of equal densities.

One can ask ourselves what the study of unequal densities had brought to us beyond what we knew already from ref. 2. Let us start with the mathematics. The two-component Burgers equations turned out to have interesting properties that can be unveiled because one can find exact weak solutions. The spectrum of velocities shown in Fig. 8 which can be obtained in the case of unequal densities only, is one example. We would like to stress that unlike the one-component Burgers equation where one knows all the solutions (this equation is “integrable”) we were able to find only a class of solutions. Is the two-component Burgers equation only “partially integrable”? This remains an open question. The problem of the stability of the solutions was also not properly studied. Another interesting problem is study of the noisy case which we didn’t touch. What we have partially learned already in the case of equal densities and more extensively in the case of unequal densities is to which incredible extend mean-field calculations are useful. This remains true if we look at “macroscopic” structures only, as seen in the case of phase separations. For example, the values of the drift velocities obtained in Section 3 from the mean-field equation describe the movement of the condensate in the stochastic process as shown in Section 1. With the proper interpretation the same drift velocities can be rediscovered in the stationary states in which we take into account fluctuations, in the two-point correlation functions (see Eq. (4.1)) or in a

combination of average quantities of one-point functions (see Eq. (4.2)). One last remark, the simple and nice expression for the current (1.7) obtained in the case of equal densities, is gone. The currents shown in Fig. 10 are obtained solving numerically transcendental equations.

Before finishing this paper we will like to comment on a paper⁽¹⁰⁾ where, in the case of equal densities, one questions the existence of the mixed phase. If one uses the grand canonical ensemble and the algebra presented in ref. 2 and two hypotheses one argues that for “cosmological” large lattices the mixed phase disappear. For example, if one takes $\lambda = 1$ and $q = 1.11$, the dimension of the lattice should be of the order 10^{70} in order to “loose” the mixed phase. If the value of q gets closer to 1 one get lattice lengths of the order 10^{490} or more. If the calculations of ref. 10 describe indeed the reality this would be a fascinating phenomenon, certainly more interesting that the model itself. In ref. 10 one has made one mathematical hypothesis which was proven correct⁽¹¹⁾ and a technical hypothesis according to which one neglects in the calculation configurations with no vacancies. This second hypothesis, which was used already in ref. 2, is probably also irrelevant.⁽¹²⁾ Our own doubt about the results of ref. 10 come from the use of the grand canonical ensemble. As stressed in ref. 2, for stochastic processes as defined for example in Section 1, there is no grand canonical ensemble. One can make an ad hoc definition, hope to be lucky and get the right results. As shown in ref. 2, for the two-point correlation functions in the mixed phase, the canonical and grand canonical ensembles give very different results (see Fig. 21). It looked however that for the one-point function (the current) the results were correct. We don’t want here to defend here the existence of the mixed phase (if it survives up to lattice lengths of the order of 10^{70} , it is enough for physical purposes), on the contrary, we think that the real challenge is to clarify the problem. One more argument in the favor of the existence of the mixed phase can be found in ref. 13 where one considers the open system (no grand canonical calculation in this case) for the same bulk parameters as those taken on the ring when one has the mixed phase. The input and output rates are chosen symmetric for the positive and negative particles. One sees a first-order phase transition between a phase where the density corresponds to the fluid (in the mixed phase on the ring) and a maximum current phase which corresponds to the condensate on the ring. (We remind the reader that the densities in the fluid depend on q and λ . Only and not on the density $p = m = \rho$).

ACKNOWLEDGMENTS

We would like to thank Oleg Zaborovsky for reading the manuscript and for useful comments. This research was supported in part by the

National Science Foundation under Grant No. PHY99-07949. VR is an ARC IREX fellow.

REFERENCES

1. P. F. Arndt, T. Heinzl, and V. Rittenberg, *J. Phys. A Math. Gen.* **31**:L45 (1998).
2. P. F. Arndt, T. Heinzl, and V. Rittenberg, *J. Statist. Phys.* **97**:1 (1999).
3. P. F. Arndt, *Phys. Rev. Lett.* **84**:814 (2000).
4. C. N. Yang and T. D. Lee, *Phys. Rev.* **87**:404 (1952).
5. N. F. Britton, *Reaction-Diffusion Equations and their Application to Biology* (Academic Press, 1986); J. D. Murray, *Mathematical Biology* (Springer 1989).
6. J. D. Logan, *An Introduction to Nonlinear Differential Equations* (John Wiley, 1994).
7. K.-t Leung and R. K. P. Zia, *Phys. Rev. E* **56**:308 (1997).
8. T. Sasamoto, *Phys. Rev. E* **61**:4980 (2000).
9. F. H. Jafarpour, cond-mat/0004357.
10. N. Rajewsky, T. Sasamoto, and E. R. Speer, *Physica A* **279**:123 (2000).
11. D. Zagier (private communication).
12. E. Levine (private communication).
13. P. F. Arndt, S. Radic, and V. Rittenberg (to be published).